View metadata, citation and similar papers at core.ac.uk

brought to you by CORE

provided by Elsevier - Publisher Connector

Autonomic Neuroscience: Basic and Clinical 166 (2012) 47–53

Contents lists available at SciVerse ScienceDirect

Autonomic Neuroscience: Basic and Clinical

journal homepage: www.elsevier.com/locate/autneu

Cardiac and pulmonary arterial remodeling after sinoaortic denervation in normotensive rats

K. Flues, I.C. Moraes-Silva, C. Mostarda, P.R.M. Souza, G.P. Diniz, E.D. Moreira, A.C. Piratello, M.L. Barreto Chaves, K. De Angelis, Vera Maria Cury Salemi, M.C. Irigoyen *, E.G. Caldini

Experimental Hypertension Laboratory, Hypertension Unit, Heart Institute, Department of Pathology, University of Sao Paulo Medical School, São Paulo, SP, Brazil

ARTICLE INFO

Article history:
Received 8 June 2011
Received in revised form 9 October 2011
Accepted 12 October 2011

Keywords:
Baroreflex
Autonomic nervous system
Hypertension
Cardiac remodeling
Pulmonary artery remodeling
Pulmonary hypertension

ABSTRACT

Blood pressure variability (BPV) and baroreflex dysfunction may contribute to end-organ damage process. We investigated the effects of baroreceptor deficit (10 weeks after sinoaortic denervation — SAD) on hemodynamic alterations, cardiac and pulmonary remodeling. Cardiac function and morphology of male Wistar intact rats (C) and SAD rats (SAD) (n = 8/group) were assessed by echocardiography and collagen quantification. BP was directly recorded. Ventricular hypertrophy was quantified by the ratio of left ventricular weight (LVW) and right ventricular weight (RVW) to body weight (BW). BPV was quantified in the time and frequency domains. The atrial natriuretic peptide (ANP), alpha-skeletal actin (α-skelectal), collagen type I and type III genes mRNA expression were evaluated by RT-PCR. SAD did not change BP, but increased BPV (11 ± 0.49 vs. 5 ± 0.3 mm Hg). As expected, baroreflex was reduced in SAD. Pulmonary artery acceleration time was reduced in SAD. In addition, SAD impaired diastolic function in both LV (6.8 ± 0.26 vs. 5.02 ± 0.21 mm Hg) and RV (5.1 ± 0.21 vs. 4.2 ± 0.12 mm Hg). SAD increased LVW/BW in 9% and RVW/BW in 20%, and augmented total collagen (3.8-fold in LV, 2.7-fold in RV, and 3.35-fold in pulmonary artery). Also, SAD increased type I (~6-fold) and III (~5-fold) collagen gene expression. Denervation increased ANP expression in LV (75%), in RV (74%) and increased α-skelectal expression in LV (300%) and in RV (546%). Baroreflex function impairment by SAD, despite not changing BP, induced important adjustments in cardiac structure and pulmonary hypertension. These changes may indicate that isolated baroreflex dysfunction can modulate target tissue damage.

© 2011 Elsevier B.V. Open access under the Elsevier OA license.

1. Introduction

Baroreceptor-mediated reflex control of circulation has been found to be an important risk predictor after cardiovascular events. Changes in baroreflex sensitivity and heart rate variability (HRV), the two main markers of autonomic nervous system activity, have been linked to an increased mortality rate, particularly in hypertensive subjects with a history of cardiovascular disease (La Rovere et al., 1998; Schwartz and La Rovere, 1998; Gerritsen et al., 2001)

Several studies have shown that reduced baroreflex sensitivity and HRV are independent markers of mortality after myocardial infarction (La Rovere et al., 1998). Moreover, decreased baroreflex sensitivity has been associated with increase in stroke events (Liu et al., 2007) and atherosclerosis development (Sasaki et al., 1994). Furthermore, it can be directly associated with cardiac remodeling and damage in human and animals (Grassi et al., 2006; Miao et al., 2006). Together, these structural changes may contribute to a loss of functional capacity of the heart. The hemodynamic and neurohumoral alterations produced by chronic sinoaortic denervation (SAD) have been studied in rats as a model of baroreflex deficit associated with increased blood pressure variability (BPV) (Miao and Su, 2002; Miao et al., 2003; Miao et al., 2004; Miao et al., 2006; Grassi et al., 2009; Hisashi et al., 2009; Kudo et al., 2009). Indeed, SAD causes a substantial increase in BPV with no change in the mean blood pressure (BP) and it is a useful method to investigate the pathology of high BPV. Some studies have reported that SAD produces various forms of end-organ damage (Su and Miao, 2001), including cardiac hypertrophy, cardiovascular remodeling, and pulmonary damage (Miao and Su, 2002; Miao et al., 2004; Tao et al., 2008). However, the pathogenesis of theses damages is yet to be fully understood, although high BPV has been acknowledged as a major contributing factor (Miao et al., 2006).

This lack of information on the relationship between baroreflex sensitivity and myocardial structural changes and pulmonary artery remodeling encouraged us to design the present study.

Our main objective was two-fold: a) to evaluate whether baroreflex dysfunction plays a role in the hypertrophy process within the normal blood pressure range, and b) to evaluate whether BPV plays a role in pulmonary hypertension.

* Corresponding author at: Heart Institute (InCor), University of Sao Paulo, Medical School, Av. Dr. Eneas de Carvalho Aguiar, 44-Bloco 1, Subsolo, Sao Paulo, SP, Brazil, ZIP CODE: 05403-000. Tel.: +55 11 30695006; fax: +55 11 30695327.
E-mail address: hipirigoyen@incor.usp.br (M.C. Irigoyen).

1566-0702 © 2011 Elsevier B.V. Open access under the Elsevier OA license.
doi:10.1016/j.autneu.2011.10.005

2. Methods

2.1. Animals

Experiments were performed in 2 month old male normotensive Wistar rats, obtained from the Animal Shelter of the Biomedical Sciences Institute (University of Sao Paulo, Sao Paulo, Brazil) and allocated at the Experimental Hypertension Laboratory Animal Shelter (Heart Institute, University of Sao Paulo, Sao Paulo, Brazil). Rats were housed in plastic cages (4 per cage) in a temperature-controlled room (22 °C) with a 12-hour dark–light cycle receiving standard chow and water *ad libitum*. All surgical procedures and protocols used were approved by the University of Sao Paulo Ethical Committee and were in accordance with National Institutes of Health Guide for the Care and Use of Laboratory Animals. The rats were randomly assigned into 2 groups (n = 8/group): normotensive control (C) and normotensive sinoaortic denervated (SAD). After 10 weeks all groups were submitted to hemodynamic and cardiac morphofunctional evaluations.

2.2. Sinoaortic denervation

Sinoaortic denervation was performed in Wistar rats at the age of 2 months according to the procedure described by Krieger (Krieger and Marseillan, 1963; Krieger, 1964). Briefly, after a 3-cm midline incision the sternocleidomastoid muscles were reflected laterally, exposing the neurovascular sheath. The common carotid arteries and the vagal trunk were isolated, and the aortic depressor fibers, either traveling with the sympathetic nerve or as an isolated aortic nerve, were cut. The communicating branch of the aortic fibers was also resected. The third contingent of aortic baroreceptor fibers traveling with the inferior laryngeal nerve was interrupted by resection of the superior laryngeal nerve after the carotid bifurcation was exposed extensively for carotid stripping. To complete SAD, the sinus nerve, all carotid branches and the carotid body were resected (Krieger and Marseillan, 1963).

2.3. Non-invasive evaluations of cardiac function

The transthoracic echocardiography was performed at the end of protocol using a SEQUOIA 512 (ACUSON Corporation, Mountain View, CA, USA). The echocardiography indexes were obtained according to the recommendations of the American Society of Echocardiography. Images were obtained in anesthetized rats (Ketamine 80 mg/kg and Xylazin 12 mg/kg, i.p.) with the transducer on each animal's shaved chest (lateral recumbence). All measurements were based on the average of 3 consecutive cardiac cycles. Wall thickness and LV dimensions were obtained from a short-axis view at the level of the papillary muscles. LV mass was calculated using the following formula, assuming a spherical LV geometry and already validated in rats: LV mass = $0.8 \times \{1.047\ [(\mathrm{LVd} + \mathrm{PWDIA} + \mathrm{IVSDIA})^3 - (\mathrm{LVd})^3]\} + 0.6$ g, where 1.047 is the specific gravity of muscle, LVd is LV end-diastolic diameter, PWDIA is end-diastolic posterior wall thickness and IVSDIA is end-diastolic interventricular septum thickness. In addition, another morphology index was evaluated — the relative wall thickness (RWT), which is expressed by $2 \times \mathrm{PWDIA}/\mathrm{LVd}$. This represents the relation between the LV cavity in diastole and the LV posterior wall (Lang et al., 2005).

Parameters of systolic function: ejection fraction (EF) and velocity of circumferential fiber shortening (VCF); parameters of diastolic function: normalized LV isovolumetric relaxation time (IVRT) and normalized peak E deceleration time (DESACE) corrected by the square root of the R–R interval. Myocardial performance index (MPI) was also evaluated (were quantified) (Wichi et al., 2007).

Pulmonary artery acceleration time (PAAT) was used as an echocardiographic (Thibault et al., 2010) indicator of pulmonary hypertension (Hardziyenka et al., 2006; Koskenvuo et al., 2010). PAAT was measured from the onset of systolic flow to peak pulmonary outflow velocity according to the American Society of Echocardiography's Guidelines and Standards Committee and the Chamber Quantification Writing Group.

2.4. Cardiovascular and autonomic assessments

2.4.1. Hemodymamics

One day after echocardiographic evaluations, two catheters (Tygon + PE10) were implanted in anesthetized rats (Ketamine 80 mg/kg and Xylazin 12 mg/kg, i.p.) into the femoral artery and vein for direct measurements of AP and drug administration, respectively. The catheters were tunneled subcutaneously and exteriorized through the back of the neck. Rats were studied 24 h after catheter placement; the rats were conscious and allowed to move freely during the experiments. The arterial cannula was connected to a strain-gauge transducer (Blood Pressure XDCR, Kent© Scientific, Litchfield, CT, USA), and AP signals were recorded over a 30-minute period by a microcomputer equipped with an analog-to-digital converter board (Windaq, 2 kHz sampling frequency, Dataq Instruments, Springfield, OH, USA) (Irigoyen et al., 2005; Souza et al., 2007). The recorded data were analyzed on a beat-to-beat basis to quantify changes in mean AP and heart rate (HR). HR variability (HRV) and systolic BPV in time domain were determined using the standard deviation of the basal recording period.

2.4.2. Baroreflex sensitivity

Baroreflex sensitivity was evaluated by a mean index relating the tachycardic and the bradycardic responses for mean AP changes (~30–40 mm Hg) induced by increasing doses of sodium nitroprusside (0.05 to 1.6 μg/kg) and phenylephrine (0.25 to 32 μg/kg) injections, respectively. Data were expressed as beats per minute (bpm) per mm Hg. Maximal volume per injection was 0.1 mL (Irigoyen et al., 2005; Souza et al., 2007).

2.4.3. Invasive evaluation of cardiac function

One day after hemodynamic evaluations, two catheters (Tygon + PE50) were implanted in anesthetized rats (pentobarbital sodium 0.1 mL/100 g, iv) into carotid artery and jugular vein and advanced to LV and RV, respectively. Pressure signals of LV and RV were measured using a transducer (Blood Pressure XDCR, Kent© Scientific, Litchfield, CT, USA) and were digitally recorded (5 min) with a data acquisition system (WinDaq, 2-kHz, DATAQ, Springfield, OH, USA). The recorded data were analyzed on a beat-to-beat basis to quantify changes in LV and RV pressure. The following indices were obtained: heart rate (HR), LV systolic pressure (LVSP), LV end-diastolic pressure (LVEDP), and maximum rate of LV pressure rise and fall ($+\mathrm{dP/dt}$ max and $-\mathrm{dP/dt}$ max), RV systolic pressure (RVSP), RV end-diastolic pressure (RVEDP), and maximum rate of RV pressure rise and fall ($+\mathrm{dP/dt}$ max and $-\mathrm{dP/dt}$ max) (Wichi et al., 2007).

2.4.4. Heart rate and blood pressure variability

Time-domain analysis consisted in calculating mean HR and systolic BP (SBP), HR variability (HRV) and SBP variability (SBPV) as the standard deviation from its respective time series.

The overall variability of the SBPV and pulse interval was assessed in the frequency domain analysis by spectral estimation. The whole 20-min time series of SAP and PI were cubic-spline-interpolated (250 Hz) and decimated to be equally spaced in time. Following linear trend removal, power spectral density was obtained by the Fast Fourier Transformation using Welch's method over 16,384 points with a Hanning window and 50% overlapping. Spectral power for low-frequency (LF: 0.20–0.75 Hz) and high-frequency (HF 0.75–3.0 Hz) bands were calculated by power spectrum density integration within each frequency bandwidth, using a customized routine (MATLAB 6.0; Mathworks, Natick, MA) (Bertagnolli et al., 2008; Heeren et al., 2009). The autonomic balance (LF/HF) was calculated by the ratio of LF and HF absolute values.

2.4.5. Tissue collection

One day after cardiovascular measurements, rats were divided into two groups. Animals were weighed and killed by decapitation.

First group: a transverse incision below the diaphragm and bilateral thoracotomy incisions were performed in the sodium pentobarbital (40 mg/kg i.p.) anesthetized rats, in order to expose the heart. A needle (40×12) was carefully introduced into the LV apex. The heart was arrested in diastole by perfusion with a NaCl 0.9% plus 14 mM KCl solution (pressure equal to a 9.56 mm Hg), followed by 10% formaldehyde for tissue fixation. Briefly, hearts and lungs were excised, trimmed, weighed and immersed in formaldehyde 4% in PBS for 24 h. Following this, LV, RV and lung were transected perpendicular to the long axis and processed and embedded in paraffin to perform histological sections. Histomorphometric analyses were performed by blinded observers. Sections of 5μm-think were stained with picrosirius red for collagen quantification (Junqueira, 1979; Piratello et al., 2010). Morphometric data were obtained from histological images made in light microscope (Leica DMR; Leica Microsystems GmbH, Wetzlar, Germany) connected to a video camera coupled to a compatible microcomputer. The images were processed using the Image-Pro Plus 6.0 for windows software (Media Cybernetics, USA). All measures were performed in histological images obtained with the 40× objective lens.

Second group: Hearts were dissected into bilateral ventricles and weighed. The ratio of left and right ventricular weight (mg) to body weight (g) was evaluated as an index of ventricular hypertrophy. Ventricles were kept at −80 °C, and used for PCR assay.

2.4.6. Real-time RT-PCR

Total RNA was obtained using the Trizol reagent (Invitrogen), following the manufacturer instructions. For reverse transcriptase, we employed 1 μg of total RNA using SuperScript II RNase H Reverse Transcriptase (Invitrogen). Real-time RT-PCR was performed using the SYBR Green PCR master mix (Invitrogen) in a thermocycler, according to manufacturer recommendations (Corbett Research, Sydney, Australia). The following primer sequences were used:

- for β-actin: 5 -AGT TCG CCA TGG ATG ACG AT-3 and 5 -AAG CCG GCC TTG CAC AT-3
- for atrial natriuretic factor (ANF): 5 -AGT GCG GTG TCC AAC ACA G-3 and 5 -CTT CAT CGG TCT GCT CGC T-3
- for skeletal α-actin: 5 -CCT GCC ACA CGC CAT CAT-3 and 5 -GCT CGG TGA GGA TTT TCA TCA G-3
- collagen type I: 5 -CGA GAC CCT TCT CAC TCC TG-3
  5 -GCA TCC TTG GTT AGG GTC AA-3
- collagen type III: 5 -TGG TTT CTT CTC ACC CTG CT-3
  5 -TCT CCA AAT GGG ATC TCT GG-3 .

Samples were run in duplicate, and the real-time RT-PCR data were normalized to β-actin gene.

2.4.7. Statistical analysis

Data are reported as mean ± SEM and Student's *t* test was used to compare means between the two groups. Pearson correlation was used to study the association between variables. The significance level was established as $p<0.05$.

3. Results

3.1. Body weight

Body weight was not different between groups at the beginning (two weeks: C: 223 ± 4 vs. SAD: 223 ± 4 g) and at the end of the protocol (10 weeks: C: 423 ± 8 vs. SAD: 421 ± 8 g).

Table 1
Hemodynamic evaluation in normotensive control (C) and normotensive SAD (SAD) groups.

Measurement/group	C	SAD
DBP (mm Hg)	89 ± 1	92 ± 3
SBP (mm Hg)	123 ± 2	125 ± 3
MBP (mm Hg)	104 ± 2	106 ± 3
HR (bpm)	313 ± 6	329 ± 3
SBP SD (mm Hg)	6 ± 0.4	9 ± 0.7*
TR (bpm/mm Hg)	2.92 ± 0.14	0.46 ± 0.07*
BR (bpm/mm Hg)	1.68 ± 0.12	0.49 ± 0.06*

Data are reported as mean ± SEM. *$p<0.05$ vs. C. Results of diastolic arterial pressure (DAP), systolic arterial pressure (SAP), mean arterial pressure (MAP), heart rate (HR), systolic arterial pressure standard deviation (SAP SD), tachycardic (TR) and bradycardic (BR) responses to AP changes.

Table 2
Heart rate and blood pressure variability in normotensive control (C) and normotensive SAD (SAD) groups.

Measurement/group	C	SAD
VAR RR (ms^2)	45 ± 7.3	45 ± 8.8
LF (ms^2)	1.30 ± 0.26	0.98 ± 0.25
HF (ms^2)	9.1 ± 1.64	6.4 ± 1.19
LF/HF	0.11 ± 0.01	0.18 ± 0.02
SBPV (mm Hg^2)	10 ± 1	57 ± 12*
LF (mm Hg^2)	1.8 ± 0.3	4.3 ± 0.6*
HF (mm Hg^2)	1.3 ± 0.2	1.8 ± 0.2
Alpha índex (ms/mm Hg)	0.91 ± 0.04	0.51 ± 0.10*

Data are reported as mean ± SEM. *$p<0.05$ vs. C. Results of spectral powers of RR interval variability (VAR RR), low frequency (LF: 0.20–.75 Hz), high frequency (HF: 0.75–3.00 Hz) bands, autonomic balance (LF/HF), and systolic blood pressure variability (SBPV).

3.2. Hemodynamic assessments

As shown in Table 1, SAD did not change BP values. However, SAD increased the systolic BPV, as expressed by standard deviation and total variance. Baroreflex sensitivity, as expected, was reduced in SAD group. Both bradycardic and tachycardic responses were reduced in SAD group (Table 1).

3.3. Heart rate and blood pressure variability

The variability of SBP in the time domain and LF of BP were increased in denervated animals. As expected, the alpha index was reduced in SAD group (Table 2).

Despite the tendency towards decreasing values of LF and HF of HRV in SAD group, there were no differences when compared with intact group. In fact, these results were reflected in no change in autonomic balance (LF/HF) (Table 2).

3.4. Non-invasive evaluation of cardiac function

Echocardiographic evaluations, performed 10 weeks after SAD, were shown in Tables 3 and 4.

Table 3
Echocardiograph morphometric parameters in normotensive control (C) and normotensive SAD (SAD) groups.

Measurement/group	C	SAD
LVDIA/BW (cm/g)	1.86 ± 0.05	1.72 ± 0.04
IVSDIA/BW (cm/g)	0.30 ± 0.01	0.33 ± 0.02
LVPWDIA/BW (cm/g)	0.30 ± 0.01	0.37 ± 0.01*
RWT (cm)	0.32 ± 0.01	0.41 ± 0.03*
LV mass/BW (mg/g)	3.53 ± 0.09	3.66 ± 0.15*

Data are reported as mean ± SEM. *$p<0.05$ vs. C. Results of LVDIA, left ventricular diastolic dimension; IVSDIA, diastolic interventricular septum; LVPWDIA, diastolic left ventricular posterior wall thickness; RWT, relative wall thickness; LV mass/BW, left ventricular mass; BW, body weight.

Table 4
Pulmonary artery acceleration time (PAAT) and echocardiograph left ventricular functional parameters in normotensive control (C) and normotensive SAD (SAD) groups.

Measurement/group	C	SAD
PAAT (ms)	40 ± 1.3	33 ± 1.0*
MPI	0.36 ± 0.012	0.51 ± 0.025*
Systolic function		
EF (%)	0.72 ± 0.08	0.63 ± 0.01*
VCF (circ/s)	0.0048 ± 0.0002	0.0058 ± 0.0004*
Diastolic function		
nIVRT (ms)	1.47 ± 0.034	1.93 ± 0.088*
nDESACE (ms)	2.28 ± 0.07	2.85 ± 0.19*

Data are reported as mean ± SEM. *p<0.05 vs. C. Results of MPI, myocardial performance index; EF, ejection fraction; VCF, velocity of circumferential fiber shortening; nIVRT, normalized isovolumetric relaxation time; nDESACE, normalized Peak E deceleration time.

Table 5
Invasive evaluations of left ventricular function in normotensive control (C) and normotensive SAD (SAD) groups.

Measurement/group	C	SAD
LVEDP (mm Hg)	5.02 ± 0.21	6.8 ± 0.26*
LV + dP/dt max (mm Hg/s)	5807 ± 399	4404 ± 206*
LV − dP/dt max (mm Hg/s)	−3796 ± 365	−2793 ± 201*
RVEDP (mm Hg)	4.2 ± 0.12	5.1 ± 0.21*
RV + dP/dt max (mm Hg/s)	1253 ± 76	1574 ± 166
RV − dP/dt max (mm Hg/s)	−927 ± 83	−1232 ± 73

Data are reported as mean ± SEM. *p<0.05 vs. C. Results of LVEDP, left ventricle end-diastolic pressure; LV + dP/dt max, maximum rate of left ventricle pressure rise; LV − dP/dt max, maximum rate of left ventricle pressure fall; RVEDP, right ventricle end-diastolic pressure; RV + dP/dt max, maximum rate of right ventricle pressure rise; RV − dP/dt max, maximum rate of right ventricle pressure fall.

SAD animals presented mild LV systolic dysfunction as observed in VCF and EF parameters. Moreover, SAD presented LV diastolic dysfunction as indicated by IVRT and DESACE. Additionally, SAD presented elevated MPI compared to intact rats.

The parameter of PAAT was reduced in SAD group, indicating pulmonary hypertension in this group (Table 3).

3.5. Invasive evaluation of cardiac function

Invasive measurements of cardiac function by LV catheterization, demonstrated diastolic impairment in SAD rats. EDP, an index of congestive heart failure, showed a significant increase in SAD rats compared with intact rats. The LV + dP/dt and LV − dP/dt max were impaired in SAD rats (Table 5).

Similarly, an impairment of RVEDP was observed in SAD rats. However, no differences were observed in RV − or + dP/dt (Table 4).

3.6. Cardiac morphometry

SAD induced LV hypertrophy, as indicated by LV/BW estimated mass by echocardiography in SAD animals (Table 3).

Echocardiographic evaluation showed that there were no differences in both LV internal dimension (cm) during diastole and thickness of interventricular septum between the two groups. However, during diastole, the posterior wall was higher in the SAD group than in the control group. In addition, the LV relative wall thickness was increased in SAD (Table 3).

SAD induced LV and RV hypertrophy, according to LVW/BW and RVW/BW index (LV: 2.35 ± 0.08, vs. 2.15 ± 0.02 and RV: 0.6 ± 0.03 vs. 0.5 ± 0.01 mg/g, respectively).

SAD induced an augment in LV and in RV collagen in SAD in relation to C rats (LV: 0.0767 ± 0.009 vs. 0.02 ± 0.01% and RV: 0.046 ± 0.006 vs. 0.017 ± 0.01%, respectively) (Figs. 3 and 4).

3.7. Real-time RT-PCR

Collagen gene expression types I and III were markedly augmented in LV in SAD rats when compared to control rats (type I: 6.81 ± 0.13 vs. 1.01 ± 0.09 and type III: 5.68 ± 0.47 vs. 0.99 ± 0.04 fold of induction, respectively). Similar results were observed in RV (type I: 3.23 ± 0.06

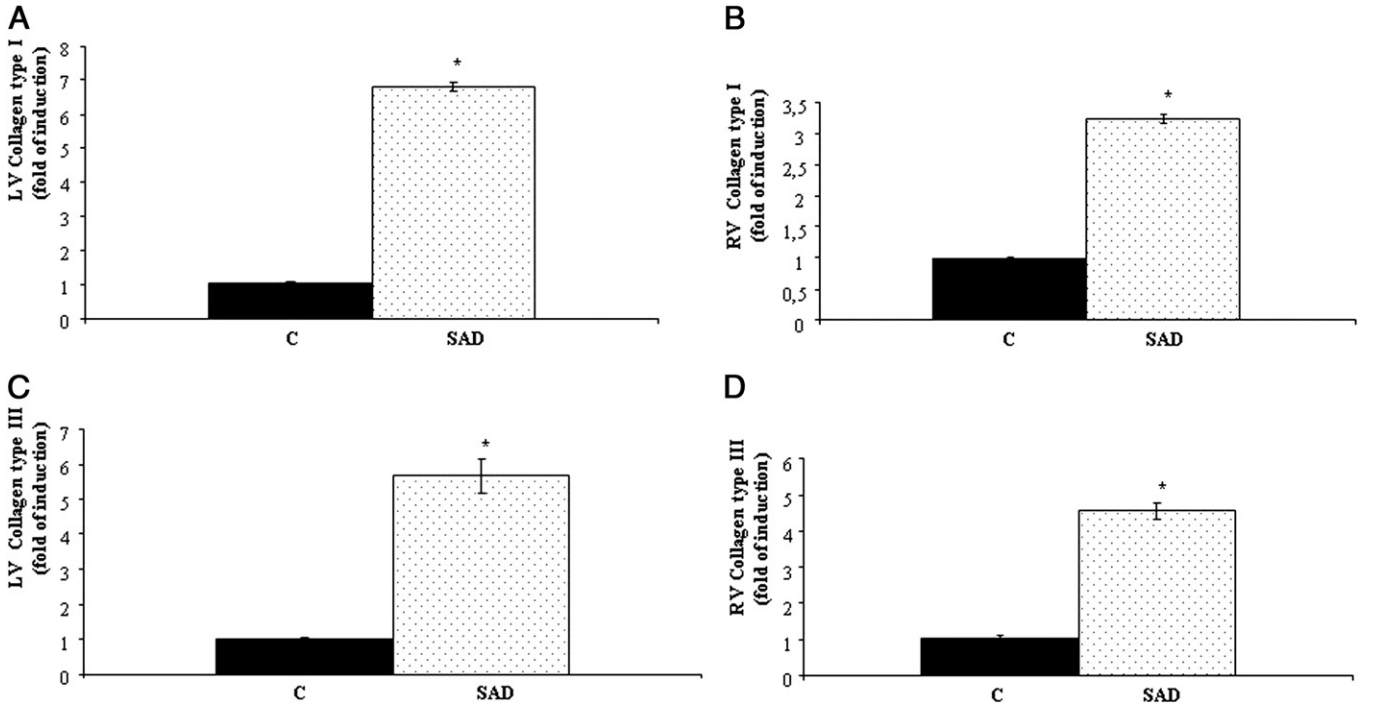

Fig. 1. (A) Collagen type I gene expression in the left ventricle, (B) collagen type I gene expression in the right ventricle, (C) collagen type III gene expression in the left ventricle, and (D) collagen type III gene expression in the right ventricle in control (C) and SAD (SAD) groups.

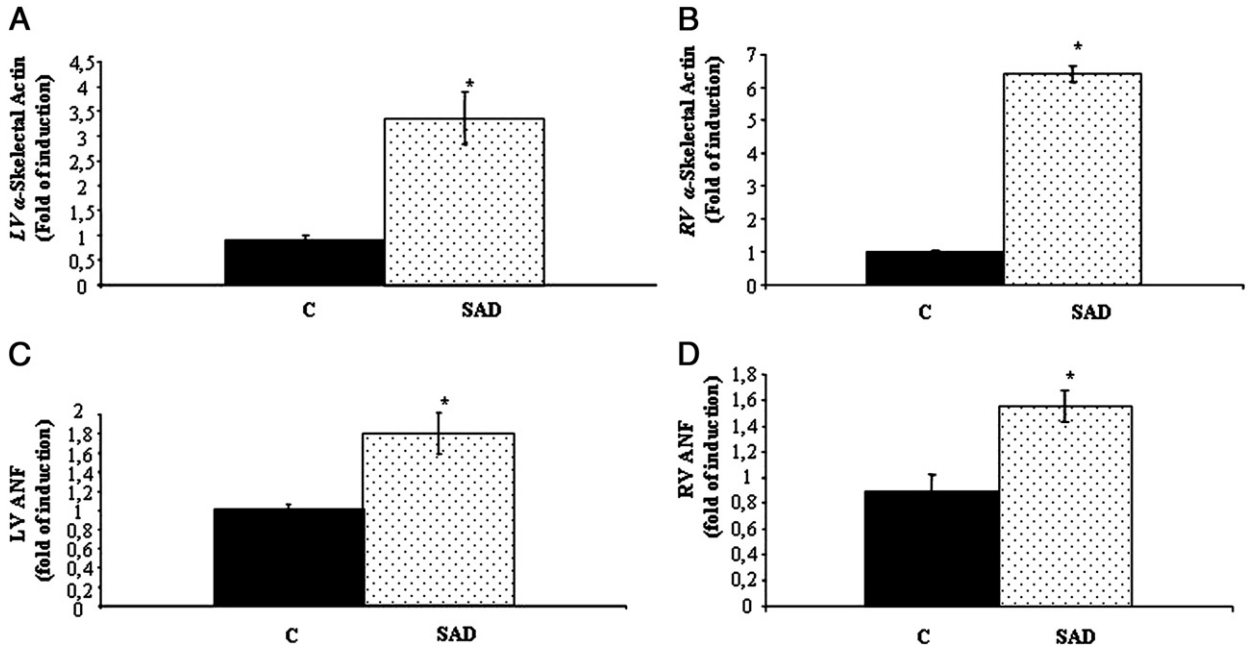

Fig. 2. (A) α-skelectal actin gene expression in the left ventricle, (B) α-skelectal actin gene expression in the right ventricle, (C) atrial natriuretic factor (ANF) gene expression in the left ventricle, and (D) atrial natriuretic factor (ANF) gene expression in the right ventricle in control (C) and SAD (SAD) groups.

vs. 0.99 ± 0.02 and type III: 4.56 ± 0.24 vs. 1.01 ± 0.1 fold of induction, respectively) (Fig. 1A, B, C, and D).

SAD enhanced atrial natriuretic factor (ANF) gene expression and α-skelectal actin gene expression in LV as compared to intact rats (ANF: 1.83 ± 0.21 vs. 1.04 ± 0.06 and α-skelectal actin gene: 3.35 ± 0.52 vs. 0.89 ± 0.10, fold of induction, respectively) (Fig. 2C and A). A similar increase was observed in RV (ANF: 1.55 ± 0.24 vs 0.89 ± 0.129 and α-skelectal actin gene: 6.4 ± 0.24 vs. 0.99 ± 0.38, fold of induction, respectively) (Fig. 2B and D).

Correlation analysis involving all studied animals showed a significant positive relationship between BPV and ANF ($r^2 = 0.72$, $p < 0.031$); BPV and collagen type I ($r^2 = 0.86$, $p < 0.007$); BPV and collagen type III ($r^2 = 0.62$, $p < 0.019$).

3.8. Collagen volume fraction evaluation in pulmonary artery

The collagen content of the medial layer of intra-acinar arteries was measured. SAD rats presented increased percentage of collagen in pulmonary artery when compared to control rats (8.85 ± 0.99 vs. 2.64 ± 0.050%).

4. Discussion

Cardiac hypertrophy is a common feature of cardiovascular diseases. Clinical and experimental studies have demonstrated that high blood pressure is a major determinant of cardiac hypertrophy in hypertension; however, several other factors contribute to the remodeling process. On the other hand, a study from Miao et al. has suggested that blood pressure variability is more important in the determination of end-organ damage than blood pressure levels (Miao et al., 2006). In the present study, our results demonstrated that baroreflex dysfunction (and the resulting changes in BPV) plays an important crucial role in the cardiac remodeling process, since denervated animals presented increased LV/BW index but similar BP levels when compared to their intact controls. The results of this study strongly suggest that, regardless of changes in BP levels, the isolated deafferentation of the baroreceptors was able to provoke cardiac hypertrophy.

SAD models are characterized by the interruption of carotid and aortic baroreceptors afferents, resulting in baroreflex dysfunction. It is worth stressing that the SAD procedure included denervation of the carotid chemoreceptors. In some studies, chemoreceptor denervation has

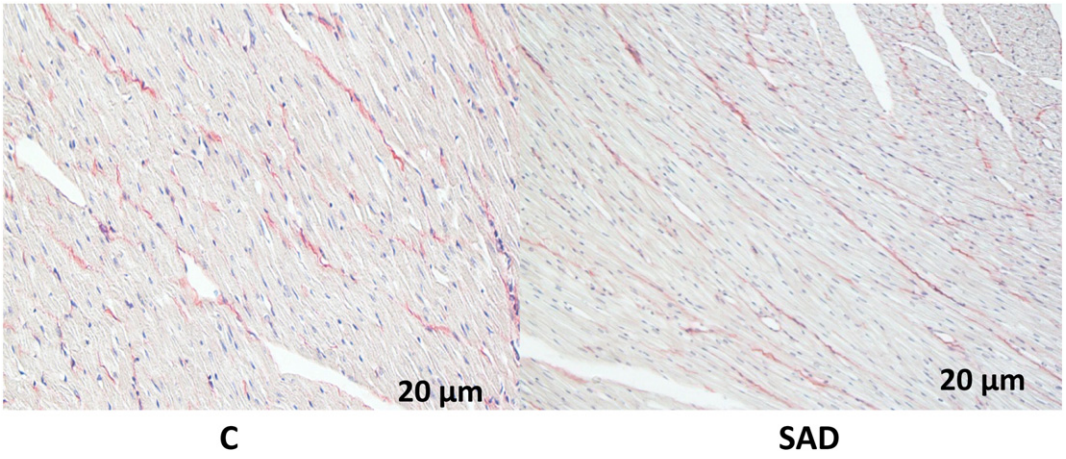

Fig. 3. Photomicrography of collagen fibers in the left ventricle in control (C) and SAD (SAD) groups.

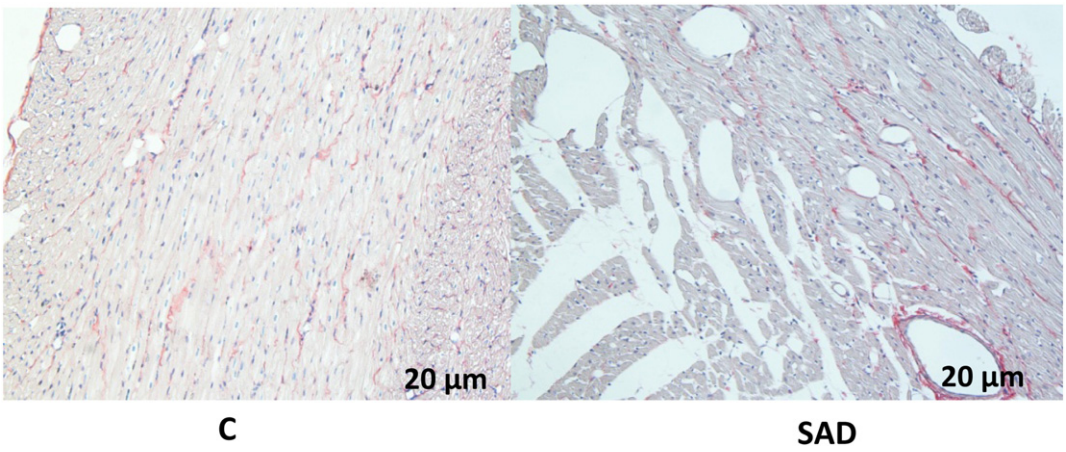

Fig. 4. Photomicrography of collagen fibers in the right ventricle in control (C) and SAD (SAD) groups.

been associated with arterial hypoxia, pulmonary hypertension, and cardiac hypertrophy (Franchini et al., 1994 and Van Vliet et al., 1999). In the study of Van Vliet et al., 1999 a complete denervation of the carotid region alone was sufficient to cause the cardiac hypertrophy, whereas the heart was unaffected by carotid denervation that spared the carotid chemoreceptors. Thus, it is possible that chemoreceptor denervation contributed to cardiac changes; however, this very same study reported that right ventricle hypertrophy was mostly influenced by chemoreceptor denervation, whereas left ventricle hypertrophy may have been a consequence of baroreflex impairment.

In this study we observed few changes in the right cardiac function, but the normotensive animals submitted to SAD were followed just for ten weeks. In longer periods of observation they might present additional changes, since the removal of the carotid body and the interruption of the laryngeal nerve represent a chronic carotid denervation procedure (O`Leary et al., 2004).

The factors influencing the cardiac hypertrophy process above discussed were quantitatively analyzed in the two groups studied: normotensive (C) and normotensive denervated (SAD) rats. Interestingly, denervation induced an increased index of hypertrophy in both LV/BW ratio and RV/BW ratio in SAD, accompanied by an increased collagen deposition when compared to intact normotensive group, indicating that denervation, solely, produced the observed structural changes.

These findings were confirmed by echocardiography data, as shown by the estimated ventricular mass, posterior wall thickness during diastole and the relative wall thickness, which is regarded as the best indicator of the remodeling process.

Which mechanisms involved in cardiac adjustments would account for the abolishment of baroreceptor function? It is well known that sinoaortic denervation increases BPV and that this is an important contributing factor to end-organ damage (Miao and Su, 2002; Agabiti-Rosei et al., 2007). Indeed, changes in heart structure have been described after performing SAD in rats. Miao and Su have described left ventricular hypertrophy in 10–16 weeks, but not in 2 weeks, and have shown that in SAD rats hypertrophy was both significantly and positively related with BPV, but not with BP level (Judy and Farrell, 1979). These data lend support to the results we obtained after 10 weeks of SAD and indicate that denervation-induced cardiac hypertrophy is a time dependent process. However, it is important to highlight that Miao and Su (2002) have found high mortality (40%) after SAD as well as a reduction of BPV during the SAD time course. In the present study, denervated animals did not die in consequence of baroreflex abolishment (data not shown).

On the other hand, cardiac functional analysis carried out through invasive and non-invasive evaluations demonstrated a sharp diastolic dysfunction and a mild systolic dysfunction in SAD rats. These results were demonstrated by enhanced end-diastolic pressure in both LV and RV resulting in a decrease in EF, increase in VCF, IVRT, nDESACE and, consequently, enhanced MPI. Although alterations in systolic function have been observed, we should emphasize that this change cannot be seen as a marker of severe systolic dysfunction, since the change we observed in this parameter was rather mild.

Furthermore, HRV and LF and HF components of HRV were similar in both groups, while the sympathetic modulation of BP (LF SBP) was increased in SAD animals. This is an important finding, since it points to another important lesion mechanism associated with SAD. In fact, the sympathetic system over activity has been repeatedly demonstrated in hypertension (Judy and Farrell, 1979). Moreover, sympathetic activity has been associated with end-organ damage and heart failure (Irigoyen et al., 1995; Brum et al., 2000; Malliani and Montano, 2002). During cardiac hypertrophy there is a cardiac myocyte gene reexpression which is expressed only during the early stages of development. This fetal reprogramming includes the reexpression of genes in ventricules, such as ANF, α-skeletal actin, and ß-myosin heavy chain. The reexpression of these fetally expressed genes is a well documented marker of a pathological cardiac hypertrophy in normal aging in many experimental models (Vikstrom et al., 1998).

The analysis of ANF, alpha-skeletal actin and collagen types I and III gene expression, is an important marker of hypertrophy and fibrosis development which may reinforce our data interpretation and the discussion carried out above. The positive and significant relationships between BPV and ANF ($r^2 = 0.72$, $p < 0.031$); BPV and collagen type I ($r^2 = 0.86$, $p < 0.007$); BPV and collagen type III ($r^2 = 0.62$, $p < 0.019$) reinforce this possibility.

Indeed, these results show that isolated baroreceptor denervation was able to induce cardiac hypertrophy in normotensive animals. Morphometric data were accompanied by an expression increase of those hypertrophy gene markers in LV and RV in SAD animals, signaling the hypertrophic stimulus.

Cardiac hypertrophy occurs as a response to a sequence of changes, including initiating signals, biochemical adjustments and regulation of gene expression. This study showed that arterial reflex dysfunction represents not only a marker of cardiovascular disease but also contributes to the progression of the disease, regardless of the final blood pressure level.

Another important finding of this study is that SAD animals presented reduced PAAT and increased RVEDP as demonstrated by non-invasive and invasive evaluations, respectively. To corroborate this finding, a significant and positive correlation between PAAT and RVEDP was found in all studied animals ($r^2 = 0.61$, $p < 0.044$); data not shown.

Additionally, SAD also presented a remodeling of the pulmonary artery wall as demonstrated by collagen deposition. All these findings suggest that the isolated baroreceptor denervation was able to induce pulmonary hypertension.

Pulmonary artery remodeling has been found to be one of the leading causes of increase in pulmonary artery pressure (Xie et al., 2010).

In conclusion, baroreflex dysfunction induces adjustments in cardiovascular structure, morphometry, genetic, hemodynamics and autonomic profile and produces alterations in pulmonary pressure. These findings may provide an opportunity to include new strategies to improve baroreflex function and to reduce BPV in the therapeutic management of the target organ in cardiovascular pulmonary diseases.

4.1. Perspectives

Baroreflex dysfunction has already been highlighted as an important prognostic marker in a range of cardiovascular conditions. Our study reinforces its importance in mediating the cardiac hypertrophy process in normotensive conditions and shed a light on the mechanisms which may be involved in the cardiac damage caused by baroreflex impairment. The observations presented in this investigation open a fruitful area for further studies regarding possible interventions which should consider the restoration of baroreflex sensitivity to normal values, in order to prevent the associated derangements.

Acknowledgements

The authors wish to thank the Fundação de Amparo a Pesquisa do Estado de São Paulo (FAPESP) for funding the present investigation, and would also like to express gratitude to Fundação Zerbini—São Paulo for supporting this study.

References

Agabiti-Rosei, E., Muiesan, M.L., Salvetti, M., 2007. New approaches to the assessment of left ventricular hypertrophy. Ther. Adv. Cardiovasc. Dis. 2, 119–128.

Bertagnolli, M., Schenkel, P.C., Campos, C., Mostarda, C.T., Casarini, D.E., Belló-Klein, A., Irigoyen, M.C., Rigatto, K., 2008. Exercise training reduces sympathetic modulation on cardiovascular system and cardiac oxidative stress in spontaneously hypertensive rats. Am. J. Hypertens. 11, 1188–1193.

Brum, P.C., Silva, G.J.J., Moreira, E.D., Ida, F., Negrão, C.E., Krieger, E.M., 2000. Exercise training increases baroreceptor gain sensitivity in normal and hypertensive rats. Hypertension 63, 1018–1022.

Franchini, K.G., Cestari, I.A., Krieger, E.M., 1994. Restoration of arterial blood oxygen tension increases arterial pressure in sinoaortic-denervated rats. Am Physiol. Soc. 0363-6135/94.

Gerritsen, J., Dekker, J.M., Ten Voorde, B.J., Kostense, P.J., Heine, R.J., Bouter, L.M., Heethaar, R.M., Stehouwer, C.D., 2001. Impaired autonomic function is associated with increased mortality, especially in subjects with diabetes, hypertension, or a history of cardiovascular disease: the Hoorn study. Diabetes Care 10, 1793–1798.

Grassi, G., Seravalle, G., Quarti-Trevano, F., Dell'Oro, R., Arenare, F., Spaziani, D., Mancia, G., 2009. Sympathetic and baroreflex cardiovascular control in hypertension-related left ventricular dysfunction. Hypertension 53, 205–209.

Hardziyenka, M., Campian, M.E., Bruin-Bon, R., Michel, M.C., Tan, H.L., 2006. Sequence of ecocardiographic changes during development of right ventricular failure in rat. Am. Soc. Echocardiogr. 19, 1272–1279.

Heeren, M., De Sousa, L., Mostarda, C., Moreira, E., Machert, H., Rigatto, K.V., Wichi, R.B., Irigoyen, M.C., De Angelis, K., 2009. Exercise improves cardiovascular control in a model of dislipidemia and menopause. Maturitas 62, 200–204.

Hisashi, K., Hisashi, K., Narimasa, T., Suguru, Y., Hidemi, K., Tsutomu, I., 2009. Large blood pressure variability and hypertensive cardiac remodeling. Circ. J. 73, 2198–2203.

Irigoyen, M.C., Moreira, E.D., Ida, F., Pires, M., Cestari, I.A., Krieger, E.M., 1995. Changes of renal sympathetic activity in acute and chronic conscious sinoaortic denervated rats. Hypertension 6, 1111–1116.

Irigoyen, M.C., Paulini, J., Flores, L.J., Flues, K., Bertagnolli, M., Moreira, E.D., Consolim-Colombo, F., Belló-Klein, A., De Angelis, K., 2005. Exercise training improves baroreflex sensitivity associated with oxidative stress reduction in ovariectomized rats. Hypertension 46, 998–1003.

Judy, W.V., Farrell, S.K., 1979. Arterial baroreceptor reflex control of sympathetic nerve activity in the spontaneously hypertensive rat. Hypertension 6, 605–614.

Junqueira, L.C., 1979. Picrosirius staining plus polarization microscopy, a specific method for collagen detection in tissue sections. Histochem. J. 4, 447–455.

Koskenvuo, J.W., Mirsky, R., Angeli, F.S., Jahn, S., Alastalo, T.P., Schiller, N.B., Boyle, A.J., Chatterjee, K., Marco, T., Yeghiazarians, Y., 2010. Int. J. Cardiovasc. Imaging 26, 509–518.

Krieger, E.M., 1964. Neurogenic hypertension in the rat. Circ. Res. 15, 511–521.

Krieger, E.M., Marseillan, R.F., 1963. Aortic depressor fibers in the rat: and electrophysiological study. Am. J. Physiol. 205, 771–774.

Kudo, H., Kai, H., Kajimoto, H., Koga, M., Takayama, N., Mori, T., Ikeda, A., Yasuoka, S., Anegawa, T., Mifune, H., Kato, S., Hirooka, Y., Imaizumi, T., 2009. Exaggerated blood pressure Variability superimposed on hypertension aggravates cardiac remodeling in rats via angiotensing II system-mediated chronic inflammation. Hypertension 54, 832–838.

La Rovere, M.T., Bigger, J.T., Marcus, F.I., Mortara, A., Schwartz, P.J., 1998. Baroreflex sensitivity and heart-rate variability in prediction of total cardiac mortality after myocardial infarction. Lancet 351, 478–484.

Lang, M.R., Bierig, M.F., Devereux, R.B., Flachskampf, F.A., Foster, E., Pellikka, P.A., Picard, M.H., Roman, M.J., Seward, J., Shanewise, J.S., Solomon, S.D., Spencer, K.T., Sutton, M.S.J., Stewart, W.J., 2005. Recommendations for Chamber Quantification: A Report from the American Society of Echocardiography's Guidelines and Standards Committee and the Chamber Quantification Writing Group, Developed in Conjunction with the European Association of Echocardiography, a Branch of the European Society of Cardiology. J. Am. Soc. Echocardiogr. 18–12.

Liu, A.J., Ma, X.J., Shen, F.M., Liu, J.G., Chen, H., Su, D.F., 2007. Arterial baroreflex: a novel target for preventing stroke in rat hypertension. Stroke 38, 1916–1923.

Malliani, A., Montano, N., 2002. Heart rate variability as a clinical tool. Ital Heart J. 8, 439–445.

Miao, C.Y., Su, D., 2002. The importance of blood pressure variability in rat aortic and left ventriculat hypertrophy produced by sinoaortic denervation. Hypertension 20, 1865–1872.

Miao, C.Y., Yuan, W.J., Su, D.F., 2003. Comparative study of sinoaortic devervated and spontaneously hypertensive rats. Am. J. Hypertens. 7, 585–591.

Miao, C.Y., Cai, G.J., Tao, X., Xie, H.H., Su, D.F., 2004. Greater hypertrophy in right than left ventricles is associated with pulmonary vasculopathy in sinoaortic-denervated Wistar–Kyoto rats. Clin. Exp. Pharmacol. Physiol. 31, 450–455.

Miao, C.Y., Xie, H.H., Zhan, L.S., Su, D.F., 2006. Blood pressure variability is more important than blood pressure level in determination of end-organ damage in rats. Hypertension 6, 1125–1135.

O`Leary, D.M., Murphy, A., Pickering, M., Jones, J.F.X., 2004. Arterial chemoreceptors in the laryngeal nerve of the rat. Respir. Physiol. Neurobiol. 137–144.

Piratello, A.C., Moraes-Silva, I., Paulini, J., Souza, P.M., Sirvente, R., Salemi, V., Flues, K., Moreira, E.D., Mostarda, C., Cunha, T., Casarine, D.E., Irigoyen, M.C., 2010. Renin angiotensin system and cardiac hypertrophy after sinoaortic denervation in rats. Clinics 65 (2), 1345–1350.

Sasaki, S., Yoneda, Y., Fujita, H., Uchida, A., Takenaka, K., Takesako, T., Itoh, H., Nakata, T., Takeda, K., Nakagawa, M., 1994. Association of blood pressure variability with induction of atherosclerosis in cholesterol-fed rats. Am. J. Hypertens. 7, 453–459.

Schwartz, P.J., La Rovere, M.T., 1998. ATRAMI: a mark in the quest for the prognostic value of autonomic markers. Autonomic Tone and Reflexes After Myocardial Infarction. Eur. Hear. J. 11, 1593–1595.

Souza, S.B., Flues, K., Paulini, J., Mostarda, C., Rodrigues, B., Souza, L.E., Irigoyen, M.C., De Angelis, K., 2007. Role of exercise training in cardiovascular autonomic dysfunction and mortality in diabetic ovariectomized rats. Hypertension 4, 786–791.

Su, D.F., Miao, C.Y., 2001. Blood pressure variability and organ damage. Clin. Exp. Pharmacol. Physiol. 9, 709–715.

Tao, X., Zhang, Y.J., Shen, F.M., Guan, Y.F., Su, D.F., 2008. Fosinopril prevents the pulmonary arterial remodeling in sinoaortic-denerveted rats by regulating phosohodiesterase. J. Cardiovasc. Pharmacol. 51, 24–31.

Thibault, H.B., Kurtz, B., Raher, M.J., Shaik, R.S., Waxman, A., Derumeaux, G., Halpern, E.F., Bloch, K.D., Scherrer-Crosbie, M., 2010. Nonivasive assessment of murine pulmonary arterial pressure: validation and application to models of pulmonary hypertension. Circ. cardiovasc. imaging 3, 157–163.

Van Vliet, B.N., Chafe, L.L., Montani, J.P., 1999. Contribution of baroreceptors and chemoreceptors to ventricular hypertrophy produced by sino-aortic denervation in rats. J. Physiol. 516 (Pt 3), 885–895.

Vikstrom, K.L., Bohlmeyer, T., Factor, S.M., Leinwand, L.A., 1998. Hypertrophy, Pathology, and Molecular Markers of Cardiac Pathogenesis. Circ. Res. 82, 773–778.

Wichi, R., Malfitano, C., Rosa, K., De Souza, S.B., Salemi, V., Mostarda, C., De Angelis, K., Irigoyen, M.C., 2007. Noninvasive and invasive evaluation of cardiac dysfunction in experimental diabetes in rodents. Cardiovasc. Diabetol. 6, 14.

Xie, L., Lin, P., Xie, H., Xu, C., 2010. Effects of atorvastatin and losartan on monocrotaline-induced pulmonary artery remodeling in rats. Clin. Exp. Hypertens. 32 (8), 547–554.